ZOOLOGICAL RESEARCH

D-dopachrome tautomerase from Japanese sea bass (*Lateolabrax japonicus*) is a chemokine-like cytokine and functional homolog of macrophage migration inhibitory factor

Feng Xu[1,2], Ming-Yun Li[2], Jiong Chen[1,2,3,*]

[1] *State Key Laboratory for Managing Biotic and Chemical Threats to the Quality and Safety of Agro-Products*, *Ningbo University*, *Ningbo*, *Zhejiang* 315211, *China*

[2] *Laboratory of Biochemistry and Molecular Biology*, *School of Marine Sciences*, *Ningbo University*, *Ningbo*, *Zhejiang* 315832, *China*

[3] *Key Laboratory of Applied Marine Biotechnology of Ministry of Education*, *Ningbo University*, *Ningbo*, *Zhejiang* 315832, *China*

ABSTRACT

D-dopachrome tautomerase (DDT), a member of the macrophage migration inhibitory factor (MIF) protein superfamily, is a newly described cytokine with chemokine-like characteristics. However, research on fish DDT remains limited. In this study, we identified a DDT homolog (LjDDT) from the Japanese sea bass, *Lateolabrax japonicus*. Sequence analysis showed that LjDDT had typical sequence features of known DDT and MIF homologs and was most closely related to DDT of rock bream (*Oplegnathus fasciatus*). *LjDDT* transcripts were detected in all tested tissues of healthy Japanese sea bass, with the highest expression found in the liver. Upon infection with *Vibrio harveyi*, *LjDDT* transcripts were significantly down-regulated in the three tested tissues, including the liver, spleen, and head kidney. Recombinant LjDDT (rLjDDT) and the corresponding antibody (anti-rLjDDT) were subsequently prepared. The administration of 100 μg/g anti-rLjDDT had a statistically significant protective effect on the survival of *V. harveyi*-infected fish. Moreover, rLjDDT was able to induce the migration of monocytes/macrophages (MO/MΦ) and lymphocytes both *in vitro* and *in vivo*, but without significant influence on the migration of neutrophils. rLjDDT exhibited chemotactic activity for lipopolysaccharide (LPS) -stimulated M1-type MO/MΦ *in vitro*, but not for cAMP-stimulated M2-type MO/MΦ. Furthermore, the knockdown of *LjCD74*, but not *LjCXCR4* , significantly down-regulated the rLjDDT-enhanced migration of MO/MΦ and relieved the rLjMIF-inhibited migration of MO/MΦ. These results indicate that LjCD74 may be the major chemotactic receptor of LjDDT and LjMIF in Japanese sea bass MO/MΦ. Combined rLjDDT+ rLjMIF treatment had no significant effect on the migration of MsiRNA, LjCD74si-, or LjCXCR4-sitreated MO/MΦ compared to the control group, suggesting that the roles of LjDDT and LjMIF may be

Received: 11 September 2019; Accepted: 06 November 2019; Online: 07 November 2019

Foundation items: This project was supported by the National Natural Science Foundation of China (31772876), Zhejiang Provincial Natural Science Foundation of China (LZ18C190001), Scientific Innovation Team Project of Ningbo (2015C110018), and K.C. Wong Magna Fund in Ningbo University

*Corresponding author, E-mail: jchen1975@163.com; chenjiong@nbu.edu.cn

DOI: 10.24272/j.issn.2095-8137.2020.003

antagonistic. In conclusion, our study demonstrates for the first time that DDT may play a role in the immune responses of fish against bacterial infection through chemotactic recruitment of MO/MΦ via mediation of CD74 as an antagonist of MIF.

Keywords: Cell migration; D-dopachrome tautomerase; Japanese sea bass; Macrophage migration inhibitory factor; Monocyte/macrophage

INTRODUCTION

Macrophage migration inhibitory factor (MIF) was first reported to inhibit the random migration of peritoneal lymphocytes and macrophages in hypersensitized guinea pigs (Bloom & Bennett, 1966; David, 1966). It is a pleiotropic proinflammatory cytokine with multiple biological functions in both innate and acquired immunity (Günther et al., 2019). MIF has chemokine-like characteristics (Bernhagen et al., 2007; Sinitski et al., 2019) and also plays a role in pathological diseases, including autoimmune diseases (Rijvers et al., 2018). MIF exerts its biological functions through autocrine and paracrine signaling via binding to and activating its receptors, including HLA class II histocompatibility antigen gamma chain (CD74), C-X-C motif chemokine receptor 4 (CXCR4), and C-X-C motif chemokine receptor 2 (CXCR2) (Bernhagen et al., 2007; Jankauskas et al., 2019; Klasen et al., 2014; Leng & Bucala, 2006; Rajasekaran et al., 2016; Rijvers et al., 2018). For example, MIF promotes the migration of B-cells through a zeta chain of the T-cell receptor-associated protein kinase 70 (ZAP70) - dependent pathway, which is mediated by the cooperative engagement of CXCR4 and CD74 (Klasen et al., 2014).

D-dopachrome tautomerase (DDT), which is a newly described cytokine and a member of the MIF protein superfamily, has attracted increasing research attention (Furukawa et al., 2016; Ma et al., 2019; Merk et al., 2012). DDT was originally identified as an enzyme in the cytoplasm of human melanoma, human liver, and rat organs, which converts D-dopachrome into 5,6-dihydroxyindole (Odh et al., 1993). The DDT gene is related to MIF in terms of sequence, enzyme activity, and gene structure (Esumi et al., 1998; Sugimoto et al., 1999). Human DDT shares 34% amino acid identity with MIF and is located within 80 kb of MIF in genomes (Merk et al., 2012). Recent studies have revealed that DDT is a functional homolog of MIF (Coleman et al., 2008; Merk et al., 2012). In mammals, DDT is associated with numerous physiological processes, including cell recruitment and migration (Rajasekaran et al., 2016; Wang et al., 2017), tumorigenesis and cancer progress (Coleman et al., 2008; Guo et al., 2016; Wang et al., 2017), and inflammatory and autoimmune diseases (Benedek et al., 2017; Fagone et al., 2018; Günther et al., 2019; Kim et al., 2017). DDT also binds to and signals via CD74 but differs from MIF by lacking the pseudo-(E)LR motif necessary for activation of chemokine receptors (Jankauskas et al., 2019; Tilstam et al., 2017; Weber et al., 2008). DDT sequences have been found in many species of fish, but studies on their biological functions are rare (Oh et al., 2013). Recombinant DDT in the rock bream (*Oplegnathus fasciatus*) induces the expression of proinflammatory cytokines such as tumor necrosis factor alpha (TNF-α), interleukin-8 (IL-8), and interleukin-1β (IL-1β) in head kidney cells, indicating that DDT may be involved in the inflammatory responses of fish (Oh et al., 2013).

The Japanese sea bass (*Lateolabrax japonicus*) is a euryhaline marine fish species commonly farmed in China, Japan, and Korea due to its high commercial value. With the growth of the marine aquaculture industry, outbreaks of infectious diseases have become increasingly frequent, leading to serious output declines and economic losses (Zhou et al., 2014). *Vibrio harveyi* has been identified as a major pathogen and cause of vibriosis disease in Japanese sea bass (Zhou et al., 2014). Studying the immune system of marine fish will provide a better understanding of their immune responses to antigenic substances and related mechanisms and may help to develop better disease management strategies for fish farmed under harsh environments. We previously found that Japanese sea bass MIF (LjMIF) can inhibit trafficking of monocytes/macrophages (MO/MΦ) and lymphocytes, enhance phagocytosis and intracellular killing of *V. harveyi* by MO/MΦ, and aggravate *V. harveyi* infection (Xu et al., 2019). In the present study, we identified a Japanese sea bass *DDT* (*LjDDT*) and investigated the relationship between *LjDDT* mRNA expression and *V. harveyi* infection. Moreover, we determined the effects of LjDDT on the regulation of immune cell trafficking and MO/MΦ function *in vitro*. The functional relationships between LjDDT and LjMIF and their receptors LjCD74 and LjCXCR4 were also investigated.

MATERIALS AND METHODS

Fish rearing

Healthy Japanese sea bass, weighing approximately 100 g, were obtained from a commercial farm in Xiangshan County, Ningbo City, China. Fish were maintained in experimental tanks filled with artificial seawater (salinity 20±2, pH 7.5±0.4, temperature 27±1 °C) and acclimated to laboratory conditions for two weeks prior to experimentation. All fish were healthy before the experiment. All experiments were performed in accordance with the Experimental Animal Management Law of China and approved by the Animal Ethics Committee of Ningbo University.

Sequence analysis of *LjDDT*

cDNA sequences of *LjDDT* were retrieved from three newly determined transcriptomes of Japanese sea bass annotated by the Beijing Genomics Institution, China (data not shown). The DDT homolog sequence was then amplified via polymerase chain reaction (PCR) using the cDNA template of Japanese sea bass and authenticated by further cloning, sequencing, and BLAST searching (http://blast.ncbi.nlm.nih.gov/Blast.cgi). The signal peptide was predicted using SignalP v4.1 (http://www.cbs.dtu.dk/services/SignalP/). The

protein domain architecture was analyzed using SMART (http://smart.emblheidelberg.de/). Multiple alignments were carried out using ClustalW (http://clustalw.ddbj.nig.ac.jp/). Non-classical secretion was analyzed using SecretomeP 2.0 (http://www.cbs.dtu.dk/services/SecretomeP/). Phylogenetic and molecular evolutionary analyses were conducted using MEGA v7 (Kumar et al., 2016). The cDNA sequences of *DDT*s or *MIF*s used in this study are listed in Supplementary Table S1.

Tissue mRNA expression analysis of *LjDDT* in Japanese sea bass under healthy and pathological conditions

In vivo bacterial challenge was performed as described previously (Xu et al., 2019). Briefly, the *V. harveyi* strain ATCC33866, which was purchased from the China General Microbiological Culture Collection Center (China), was cultured in Tryptic Soy Broth (TSB) medium at 28 °C with constant shaking at 200 r/min until the logarithmic growth phase. The harvested *V. harveyi* cells were washed three times and resuspended in 100 μL of sterile phosphate buffered saline (PBS). The experimental groups were infected by an intraperitoneal (ip) injection of *V. harveyi* (5×10^6 colony-forming units (CFU) per fish), according to the determined 50% lethal dose (LD_{50}) in 72 h; the same volume of PBS was used for the control group. The liver, spleen, and head kidney were collected from fish at 6, 12, 24, 36, and 48 h post infection (hpi) for pathology-related mRNA expression analysis using quantitative real-time PCR (qRT-PCR). The liver, spleen, head kidney, trunk kidney, gill, intestine, brain, skin, muscle, and heart of healthy Japanese sea bass were also collected for tissue mRNA expression pattern analysis using qRT-PCR.

DNase I digestion and first-strand cDNA synthesis were conducted as reported previously (Chen et al., 2019). Based on the cDNA sequence of *LjDDT*, primers LjDDT-F(+): 5'-AAACCAGAGGACAGGATGAATC-3' and LjDDT-R(-): 5'-CACACCGATAGCAGACACC-3' were designed for the detection of the *LjDDT* transcript by qRT-PCR. Amplification was performed using TB Green Premix Ex Taq II (Takara Bio, Japan), and the reaction mixture was incubated in an ABI StepOne Real-Time PCR System (Applied Biosystems, USA) as follows: 94 °C for 180 s, 40 cycles of 94 °C for 30 s, 60 °C for 30 s, 72 °C for 30 s, followed by melting curve analysis at 94 °C for 30 s, 72 °C for 30 s, and 94 °C for 30 s. Relative expression of *LjDDT* was normalized to that of *Lj18S* rRNA. Samples obtained under healthy and pathological conditions were assessed using the $2^{-\Delta CT}$ and $2^{-\Delta\Delta CT}$ methods, respectively. Each experiment was performed in triplicate and repeated four times.

Prokaryotic expression of LjDDT and antibody preparation

Primer pair LjDDT-p(+): 5'-GGAATTCATGCCTTTCATCAACT TAGAGAG-3' (underlined section is restriction site for *Eco*R I) and LjDDT-p(-): 5'-GCTCGAGTCACAAGAAGCTCATGACGG T-3' (underlined section is restriction site for *Xho* I) was designed for amplification of the complete open reading frame (ORF) sequence of LjDDT. After restriction enzyme digestion, the amplicon was cloned into the *Eco*R I/*Xho* I-digested pET-28a (+) expression vector for the construction of plasmid pET-28a-LjDDT. pET-28a-LjDDT was subsequently transformed into the *Escherichia coli* strain BL21 (DE3). The overexpression of recombinant LjDDT (rLjDDT) was induced by isopropyl-β-D-thiogalactopyranoside (IPTG). rLjDDT was purified using a nickel-nitrilotriacetic acid (Ni-NTA) column (QIAGEN, China) at 4 °C. Lipopolysaccharide (LPS) was removed using Detoxi-Gel (Thermo Fisher Scientific, USA). The purified rLjDDT was then used as an antigen to immunize mice to produce antiserum. The anti-rLjDDT IgG (anti-rLjDDT) and isotype IgG (IsoIgG) were purified from mouse sera using Protein G HP SpinTrap columns (GE Healthcare, USA) and their concentrations were determined using the Bradford protein assay. The specificity of the antibody was tested by Western blotting and visualized using an enhanced chemiluminescence (ECL) kit (Advansta, USA), as described previously (Ren et al., 2019). The lyophilized rLjDDT and anti-rLjDDT were kept at –20 ºC until use.

Fish survival assay

Healthy fish were randomly divided into eight groups for survival study: i.e., (1) Control, ip-injected with 100 μL of PBS 30 min post *V. harveyi* (1×10^4 CFU/fish) infection; (2) ip-injected with rLjDDT (1 μg/g body weight) 30 min post *V. harveyi* (1×10^4 CFU/fish) infection; (3) ip-injected with rLjDDT (10 μg/g body weight) 30 min post *V. harveyi* (1×10^4 CFU/fish) infection; (4) ip-injected with rLjDDT (100 μg/g body weight) 30 min post *V. harveyi* (1×10^4 CFU/fish) infection; (5) ip-injected with anti-rLjDDT (1 μg/g body weight) 1 h before *V. harveyi* (1×10^4 CFU/fish) infection; (6) ip-injected with anti-rLjDDT (10 μg/g body weight) 1 h before *V. harveyi* (1×10^4 CFU/fish) infection; (7) ip-injected with anti-rLjDDT (100 μg/g body weight) 1 h before *V. harveyi* (1×10^4 CFU/fish) infection; and (8) ip-injected with IsoIgG (10 μg/g body weight) 1 h before *V. harveyi* (1×10^4 CFU/fish) infection. Over the next 9 d, the fish were monitored daily for death or moribund state. The Kaplan-Meier method was used to analyze the 9 d survival rate.

Isolation of MO/MΦ, lymphocytes, and neutrophils from peripheral blood

MO/MΦ, lymphocytes, and neutrophils were separated from caudal vein blood of healthy Japanese sea bass according to a previously described method (Liu et al., 2018). Briefly, heparinized blood was collected, and cells were isolated following sedimentation with 6% dextran T 500 (Sigma, USA). After low-speed centrifugation at 400 *g* for 25 min at 24 °C, cells packed below Ficoll-Hypaque PREMIUM (GE Healthcare) (i. e., erythrocytes and neutrophils) were subjected to hypotonic lysis with ice-cold ACK (Ammonium-Chloride-Potassium) Lysis Buffer (0.15 mol/L NH_4Cl, 0.01 mol/L $KHCO_3$, 0.1 m mol/L EDTA) to eliminate red blood cells. The resulting neutrophil suspension was washed and suspended in RPMI 1640 medium (Invitrogen, China). The buffer layer above the Ficoll-Hypaque PREMIUM was collected and washed carefully, and the number of cells was

determined using a hemocytometer (Sangon, China). Cells were cultured in 35 mm dishes for 12 h, and adherent MO/MΦ and non-adherent lymphocytes were carefully collected and cultured in complete medium (RPMI 1640 supplemented with 5% (v/v) Japanese sea bass serum, 5% (v/v) fetal bovine serum (FBS, Invitrogen), 100 U/mL penicillin, and 100 μg/mL streptomycin) at 24 °C with 5% CO_2.

Primary culture of Japanese sea bass head kidney-derived MO/MΦ

Head kidney-derived MO/MΦ were isolated from healthy Japanese sea bass and cultured as described previously (Chen et al., 2014). Briefly, leukocyte-enriched fractions were obtained from the Ficoll-medium interface using a Ficoll density gradient (1.077±0.001 g/mL) (Invitrogen) and seeded into 35 mm dishes. After overnight incubation at 24 °C, non-adherent cells were removed by washing and adherent cells were subsequently cultured in complete medium at 24 °C with 5% CO_2.

***In vitro* cell migration assay**

In vitro cell migration assay was performed in a 24-well Transwell chamber (Corning, USA). For the assay of peripheral blood-derived cells, rLjDDT or rLjMIF in complete medium was added to the lower chambers at concentrations of 0, 1.0, and 10.0 μg/mL respectively; MO/MΦ, neutrophils, or lymphocytes were plated on the upper chambers. The chambers were incubated at 24 °C for 4 h. Cells that migrated from the upper to lower chambers were counted using light microscopy (Nikon, Japan). Each migration assay was performed in quadruplicate.

For the polarized MO/MΦ assay, the isolated Japanese sea bass head kidney-derived MO/MΦ were treated with 10.0 μg/mL LPS or 0.5 mg/mL cyclic adenosine monophosphate (cAMP) for 12 h to produce M1 or M2 type MO/MΦ, as described previously (Chen et al., 2018). The *in vitro* chamber assay was then used to determine the chemotactic effect of rLjDDT (at concentrations of 0, 1.0, and 10.0 μg/mL, respectively) on M1 and M2 MO/MΦ, with non-stimulated MO/MΦ used as the control.

***In vivo* cell migration assay**

Fish in the experimental groups were ip-injected with 1.0 μg/g or 10.0 μg/g rLjDDT or rLjMIF per fish in 100 μL of PBS; fish in the control group received the same volume of PBS. Peritoneal cells were collected at 24 hpi and rinsed with 2 mL of PBS using a single-use aseptic injector. After centrifugation at 800 *g* for 8 min at 24 °C, cell pellets were retained and resuspended in 1 mL of PBS. The direct cell counts were evaluated at 400× magnification using a hemocytometer. MO/MΦ, lymphocytes, and neutrophils were further identified microscopically via the Wright-Giemsa staining technique according to previously described methods (Yu et al., 2019).

***In vitro* MO/MΦ migration after *LjCD74* and *LjCXCR4* knockdown**

Japanese sea bass head kidney-derived MO/MΦ were transfected with LjCD74 (MK605507) small interfering RNA (LjCD74si) (5'-GCUCCAAUGAGGAUGCAAATT-3') or LjCXCR4 (MK605474) siRNA (LjCXCR4si) (5'-CCAACACUCCAGGAUCAUUTT-3') for 48 h to knock down the expression of the target gene, with Mismatched siRNA (MsiRNA) (5'-UUCUCCGAACGUGUCACGUTT-3') treatment used as the negative control. qRT-PCR was used to confirm knockdown of LjCD74 and LjCXCR4 expression. These MO/MΦ were then plated on the upper chambers, and rLjDDT (or rLjMIF) in complete medium was added to the lower chambers at a concentration of 10.0 μg/mL. The *in vitro* cell migration assay was performed as described in the previous section.

Statistical analysis

All data are presented as mean±standard error of mean (*SEM*). Statistical analysis was performed using one-way analysis of variance (ANOVA) with SPSS v13.0 (SPSS Inc., Chicago, USA). A P -value of <0.05 were considered statistically significant.

RESULTS

Sequence analysis of LjDDT

The cDNA sequence of LjDDT, 962 nucleotides (nts) in length, was deposited in the GenBank Data Library under accession No. MH988689. The sequence contained a large ORF of 357 nts, which encoded a 118 amino acid (aa) polypeptide with a calculated molecular weight (MW) of 12.7 kDa and a theoretical isoelectric point (pI) of 6.81. Sequence analysis revealed that LjDDT had no signal peptide (Figure 1A) and may be secreted through a non-classical mode (Supplementary Figure S1). Multiple alignments revealed that LjDDT had characteristic features of known DDT proteins. LjDDT contained the "CXXC" motif at aa position 54–57 and three conserved active site residues, Pro2, Lys33, and Ile65 (Figure 1A). LjDDT showed a similar structure to that of LjMIF (Figure 1B).

Sequence comparison revealed that *LjDDT* shared the highest nucleotide identity (90.76%) with rock bream *DDT*. Phylogenetic tree analysis showed that teleost fish *DDT*s grouped together to form a distinct subcluster closely related to the subcluster of higher vertebrate *DDT*s; LjDDT was most closely related to the rock bream homolog (Figure 2; Supplementary Figure S2); the DDT and MIF clusters were distantly related (Supplementary Figure S2).

Analysis of *LjDDT* mRNA expression in healthy and *V. harveyi*-infected Japanese sea bass

The mRNA expression levels of *LjDDT* in the tissues of healthy and *V. harveyi*-infected Japanese sea bass were investigated by qRT-PCR. In healthy fish, the *LjDDT* transcript was detected in all tested tissues, including the liver, spleen, trunk kidney, gill, intestine, brain, head kidney, heart, skin, and muscle, with the highest level detected in the liver, followed by the spleen and trunk kidney (Figure 3A). Upon *V. harveyi* infection, *LjDDT* transcripts were substantially down-regulated at 12 hpi or later in the liver, at 12 and 24 hpi in the head kidney, and at 6 hpi or later in the spleen (Figure 3B–D). The

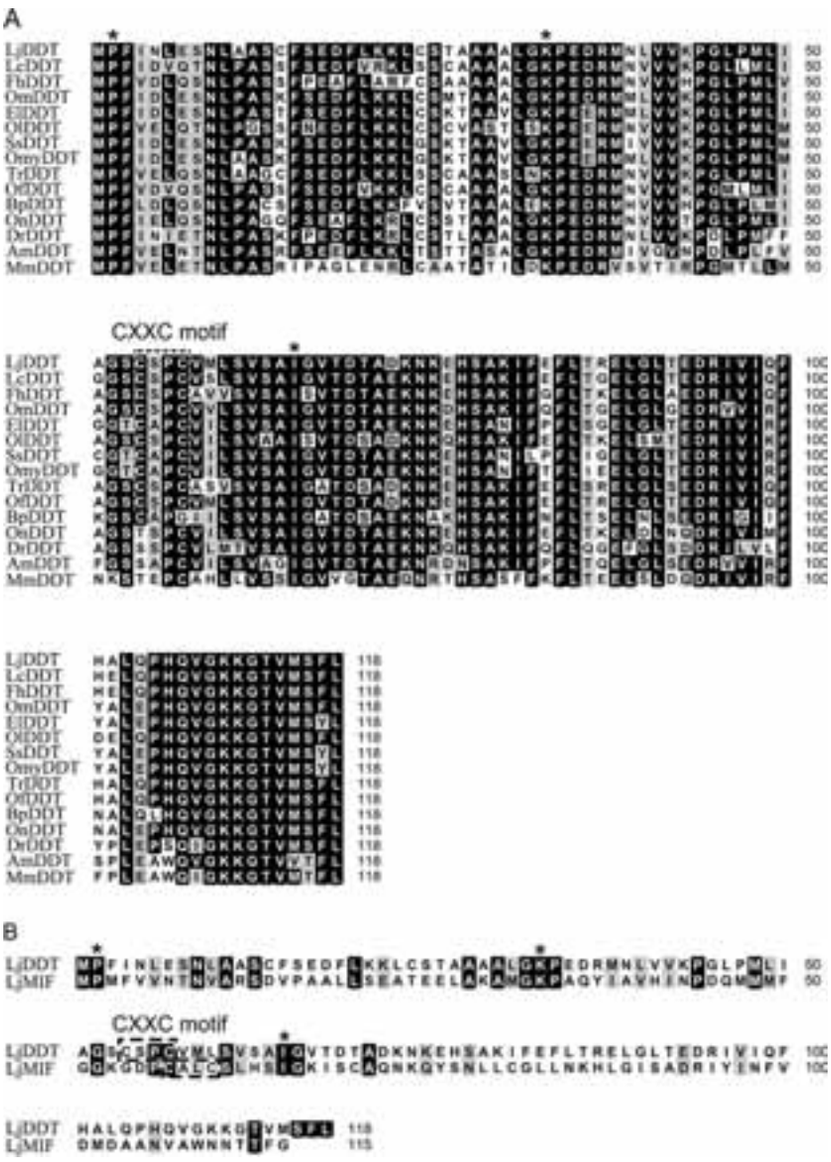

Figure 1 Multiple alignments of amino acid sequences of LjDDT with other DDT homologs (A) or LjMIF (B)

Threshold for shading was >60%, with similar residues shaded gray and identical residues shaded black. LjDDT: Japanese sea bass DDT; LcDDT: Large yellow croaker DDT; FhDDT: Mummichog DDT; OmDDT: Rainbow smelt DDT; ElDDT: Northern pike DDT; OlDDT: Japanese ricefish DDT; SsDDT: Atlantic salmon DDT; OmyDDT: Rainbow trout DDT; TrDDT: Tiger puffer DDT; OfDDT: Rock bream DDT; BpDDT: Mudskipper DDT; OnDDT: Nile tilapia DDT; DrDDT: Zebrafish DDT; AmDDT: Mexican tetra DDT; MmDDT: Mouse DDT; LjMIF: Japanese sea bass MIF. GenBank accession Nos. of sequences used are listed in Supplementary Table S1. Active site residues Pro, Lys, and Ile are marked with"*". "CXXC"motif is denoted with dotted box.

most significant *LjDDT* down-regulation was observed in the spleen at 36 hpi (0.31-fold) (Figure 3C).

Preparation of rLjDDT and corresponding antibody

After induction by IPTG, the recombinant Japanese sea bass DDT (rLjDDT) was overexpressed in *E. coli* BL21 (DE3). The MW of rLjDDT obtained from SDS-PAGE analysis was approximately 15 kDa, similar to the MW estimated from the sequence (12.7 kDa LjDDT plus 2.2 kDa His-tag) (Figure 4A). Western blot analysis revealed that the MW of native LjDDT in the serum and liver of Japanese sea bass was approximately 13 kDa, similar to the MW calculated from the sequence (12.7 kDa) (Figure 4B).

Effect of rLjDDT and anti-rLjDDT on survival rate of *V. harveyi*-infected Japanese sea bass

The 9 d survival rate experiment investigated the effects of rLjDDT and anti-rLjDDT on *V. harveyi*-infected Japanese sea

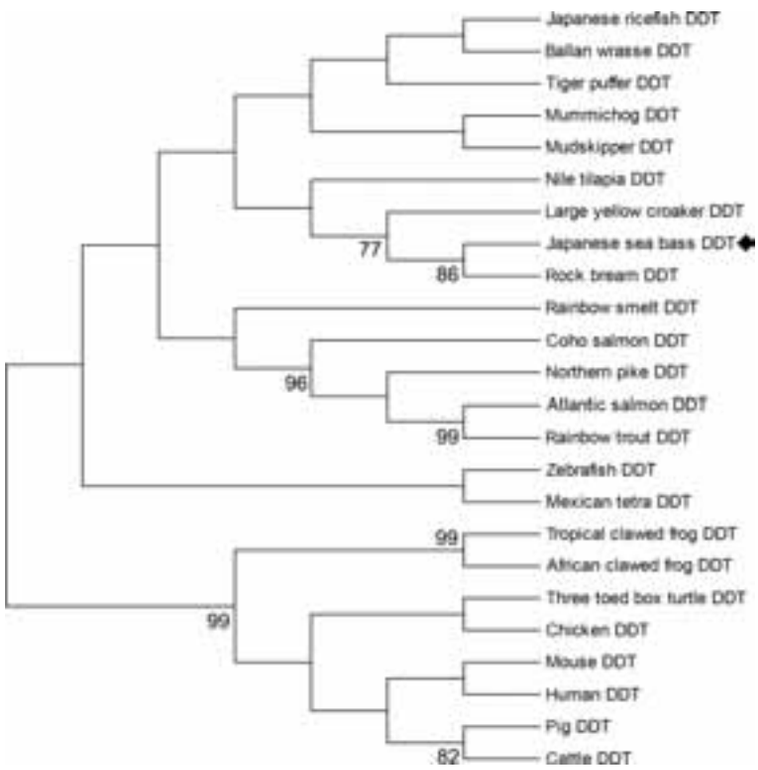

Figure 2 Phylogenetic tree of *DDT* nucleotide using neighbor-joining method (1 000 bootstrap replicates; maximum composite likelihood model) in MEGA v7

Site of Japanese sea bass *DDT* is marked with"◆". Values at forks indicate percentage of trees in which this grouping occurred after bootstrapping (1 000 replicates; shown only when >60%). Scale bar shows number of substitutions per base. GenBank accession Nos. of sequences used are listed in Supplementary Table S1.

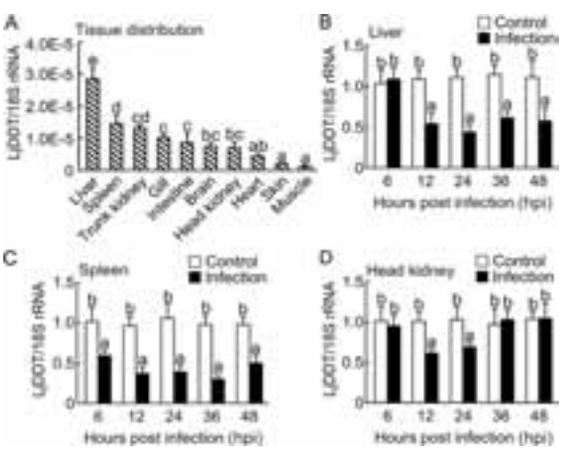

Figure 3 mRNA expression analysis of *LjDDT* in tissues of healthy (A) and *V. harveyi*-infected Japanese sea bass (B–D)

A: *LjDDT* mRNA expression level relative to that of *Lj18S* rRNA, calculated using $2^{-\Delta CT}$ method. B–D : Tissues were collected at different time points after bacterial infection. *LjDDT* mRNA expression levels relative to that of *Lj18S* rRNA were calculated using $2^{-\Delta\Delta CT}$ method. Data are expressed as mean±*SEM* of results from four fish. Values denoted by different letters are significantly different when compared by ANOVA (*P*<0.05).

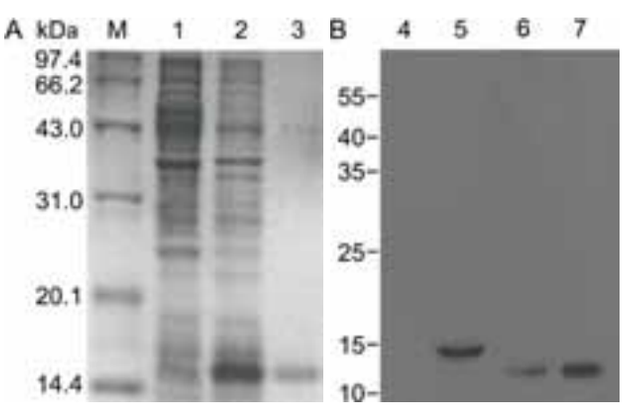

Figure 4 Prokaryotic expression and Western blot analysis of LjDDT

A: 12% SDS-PAGE analysis of bacterial lysates and purified rLjDDT. Lane M: protein marker; Lane 1: pET-28a-LjDDT/BL21 before IPTG induction; Lane 2: pET-28a-LjDDT/BL21 after IPTG induction; Lane 3: Purified rLjDDT. B: Western blot analysis of rLjDDT and native LjDDT in liver of Japanese sea bass. Lane 4: pET28a-LjDDT/BL21 before IPTG induction, negative control; Lane 5: Purified rLjDDT; Lane 6: Japanese sea bass serum; Lane 7: Japanese sea bass liver lysates.

bass. Compared with the IsoIgG-treated group, fish administered with 10 μg/g or 100 μg/g anti-rLjDDT achieved a survival rate of 20% and 43.3%, respectively, at 9 d post infection (dpi), but only 100 μg/g anti-rLjDDT showed statistical significance (Figure 5). The administration of 100 μg/g rLjDDT accelerated the death of *V. harveyi*-infected fish, and all fish died at 7 dpi (Figure 5). Fish in the other five groups all died at 9 dpi (Figure 5).

***In vitro* chemotaxis assay of rLjDDT on different cells**

In vitro transwell cell migration assay was conducted to test the chemotactic activity of rLjDDT and rLjMIF on MO/MΦ, lymphocytes, and neutrophils isolated from Japanese sea bass peripheral blood. Results showed that rLjDDT promoted the migration of MO/MΦ and lymphocytes in a dose-dependent manner (Figure 6A, B), but had no effect on the migration of neutrophils (Figure 6C). Migration of MO/MΦ and lymphocytes was also inhibited by rLjMIF in a dose-dependent manner (Figure 6A, B), but had no effect on the migration of neutrophils (Figure 6C). The administration of rLjDDT combined with equivalent rLjMIF showed no significant effect on cell migration compared with the negative control (Figure 6A–C).

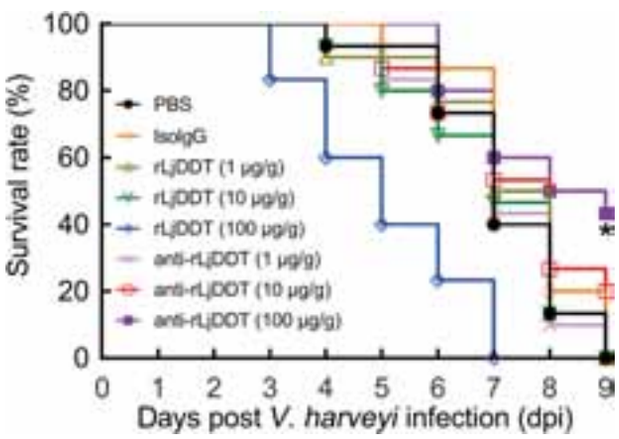

Figure 5 Effect of LjDDT on survival rate of *V. harveyi*-infected Japanese sea bass

Fish were ip-injected with equal volumes of rLjDDT, IsoIgG, or anti-rLjDDT, respectively, 30 min after *V. harveyi* infection (1×10^4 CFU/fish) or 1 h before *V. harveyi* infection (1×10^4 CFU/fish). Control group received an equal volume of PBS. Fish mortality was monitored daily for 9 d. n=30.

***In vivo* chemotaxis assay of rLjDDT on different cells**

The numbers of migrated MO/MΦ, lymphocytes, and neutrophils in the abdominal cavity of Japanese sea bass were investigated 24 h after administration of rLjDDT and rLjMIF. rLjDDT administration induced a substantial increase in MO/MΦ (10.0 μg/g) and lymphocyte (1.0 or 10.0 μg/g) numbers in the abdominal cavity of Japanese sea bass compared with the control; no obvious change in neutrophil number was observed (Figure 7A–C). rLjMIF administration had no significant effect on MO/MΦ, lymphocyte, or neutrophil numbers in the abdominal cavity of Japanese sea bass compared with the negative control (Figure 7A–C). Only the administration of 10.0 μg/g rLjDDT+rLjMIF combined induced a substantial increase in MO/MΦ numbers in the abdominal cavity of Japanese sea bass compared with the negative control (Figure 7A–C).

***In vitro* effect of rLjDDT on migration of LPS- or cAMP-stimulated MO/MΦ**

MO/MΦ polarization plays an important role in modulating proinflammatory responses in fish (Lu & Chen, 2019). The *in vitro* effect of rLjDDT on the migration of LPS- or cAMP-stimulated MO/MΦ was also determined. LPS- or cAMP-stimulation induced M1 and M2 polarization of Japanese sea bass MO/MΦ, respectively, with the up-regulation of iNOS (M1) and arginase activity (M2) (Figure 8A, B). rLjDDT promoted the migration of LPS-stimulated MO/MΦ (12.4% cells for 1.0 μg/mL rLjDDT, 15.3% cells for 10.0 μg/mL rLjDDT), whereas the random migration of LPS-stimulated MO/MΦ was 5.9% (Figure 8C). However, rLjDDT had no substantial effect on the migration of cAMP-stimulated MO/MΦ (Figure 8D).

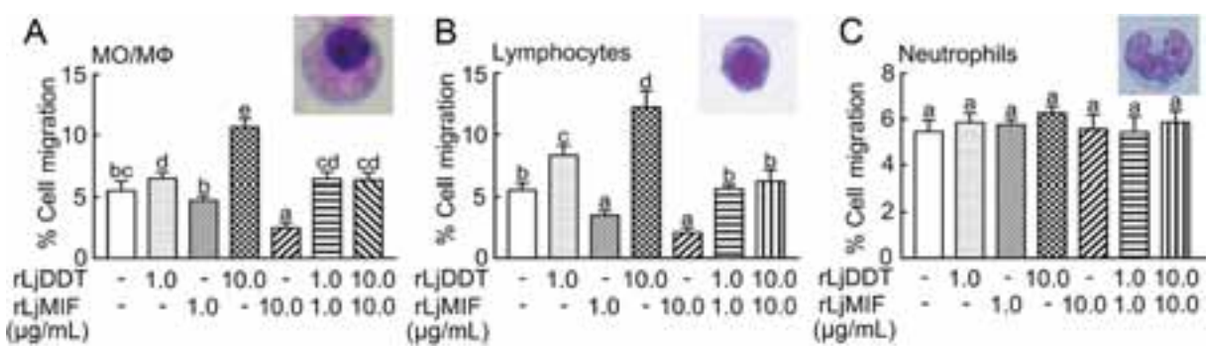

Figure 6 *In vitro* effect of rLjDDT and rLjMIF on migration of MO/MΦ (A), lymphocytes (B), and neutrophils (C) at different concentrations (0, 1.0, and 10.0 μg/mL, respectively)

Cells were counted under a light microscope at 400× magnification. Data are expressed as mean±*SEM*. n=4. Values denoted by different letters are significantly different when compared by ANOVA (P< 0.05).

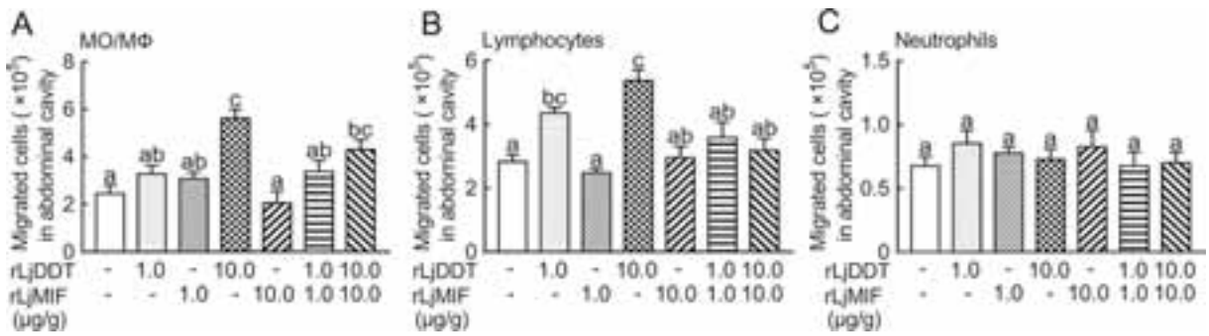

Figure 7 ***In vivo*** **effect of rLjDDT and rLjMIF administration on MO/MΦ (A), lymphocyte (B), and neutrophil (C) numbers in abdominal cavity of Japanese sea bass at different concentrations (0, 1.0, and 10.0 μg/g respectively)**

Cells were counted under a light microscope at 400× magnification 24 h after administration of rLjDDT and rLjMIF. Data are expressed as mean± *SEM*. *n*=4. Values denoted by different letters are significantly different when compared by ANOVA (*P*<0.05).

Effects of *LjCD74* and *LjCXCR4* knockdown on rLjDDT and rLjMIF-induced migration of MO/MΦ

As CD74 and CXCR4 are considered receptors of DDT in mammals (Fagone et al., 2018; Klasen et al., 2014), we determined whether *LjCD74* and *LjCXCR4* knockdown influenced rLjDDT-induced migration of MO/MΦ. We first used RNAi to knock down the expression of *LjCD74* and *LjCXCR4* in Japanese sea bass MO/MΦ. When MO/MΦ were transfected with LjCD74si or LjCXCR4si, the mRNA expression of *LjCD74* and *LjCXCR4* decreased to 23.38%± 8.05% and 21.79%±4.44%, respectively, of the normal control at 48 h (Figure 9A, B), suggesting that *LjCD74* and *LjCXCR4* were effectively knocked down by LjCD74si and LjCXCR4si, respectively. The transfection of MsiRNA had no obvious effect on *LjCD74* or *LjCXCR4* expression (Figure 9A, B). We next used LjCD74si and LjCXCR4si to explore whether *LjCD74* and *LjCXCR4* mediated the effect of LjDDT on MO/MΦ migration. After transfection with MsiRNA, 11.02% and 2.04% of MO/M Φ migrated to the lower chambers containing 10.0 μg/mL rLjDDT and rLjMIF, respectively (Figure 9C). Only 6.13% of MO/MΦ migrated to the lower chambers

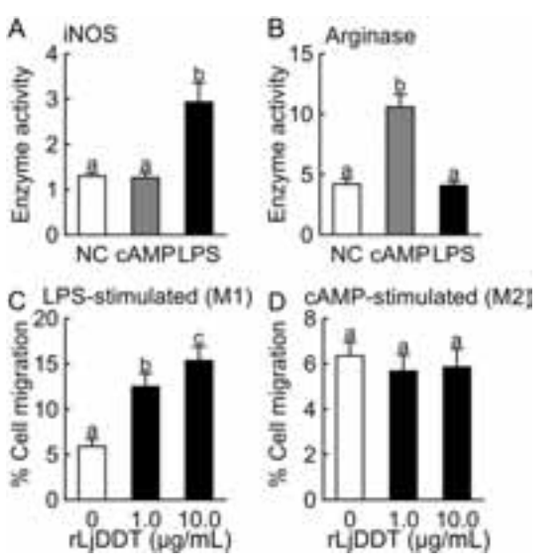

Figure 8 Effect of rLjDDT on migration of polarized Japanese sea bass MO/MΦ

LPS and cAMP were used to induce M1 and M2 polarization of MO/MΦ, respectively. Activities of iNOS (A) and arginase (B) were determined. After incubation with rLjDDT for 4 h, migration percentage of LPS- (C) or cAMP- (D) stimulated MO/MΦ was determined. Non-stimulated resting MO/MΦ were used as negative control (NC). Data are expressed as mean±*SEM*. *n*=4; Values denoted by different letters are significantly different when compared by ANOVA (*P*<0.05).

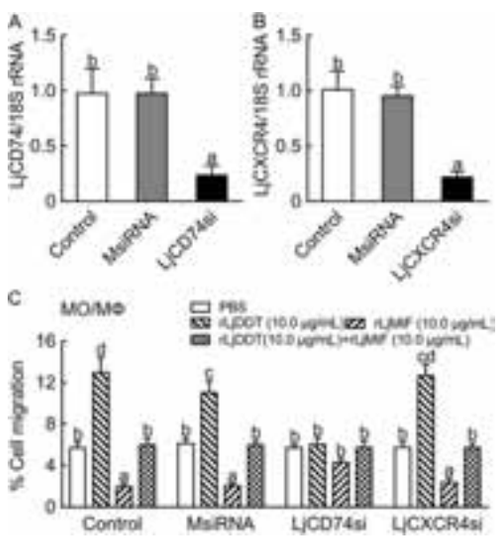

Figure 9 Effect of *LjCD74* and *LjCXCR4* knockdown on rLjDDT and rLjMIF-induced migration of MO/MΦ, respectively

Histogram displays effect of *LjCD74* (A) and *LjCXCR4* (B) siRNA transfection on knockdown of MO/MΦ *LjCD74* and *LjCXCR4* mRNA expression by RT-qPCR analysis. C: Migration percentage of Japanese sea bass MO/MΦ was examined in a Transwell chamber in presence or absence of 10.0 μg/mL rLjDDT, rLjMIF, or rLjDDT+rLjMIF combined. Each bar represents mean±*SEM*, *n*=4. Values denoted by different letters are significantly different when compared by ANOVA (*P*<0.05).

without rLjDDT or rLjMIF (Figure 9C). After knockdown of *LjCD74*, approximately 6.01% and 4.27% of the MO/MΦ migrated to the lower chambers containing 10.0 μg/mL rLjDDT and rLjMIF, respectively, compared to 5.74% in the group treated with 10.0 μg/mL rLjDDT+rLjMIF combined (Figure 9C). After knockdown of *LjCXCR4* , 12.63% and 2.36% of the MO/MΦ migrated to the lower chambers containing 10.0 μg/mL rLjDDT and rLjMIF, respectively, compared to 5.71% in the group treated with 10.0 μg/mL rLjDDT+rLjMIF combined (Figure 9C).

DISCUSSION

As a second member of the MIF superfamily, DDT is involved in various pathological roles in inflammatory, autoimmune, and chronic respiratory mammalian diseases (Günther et al., 2019; Jankauskas et al., 2019; Sinitski et al., 2019). It is clear that DDT and MIF are pleiotropic cytokines in mammals, which not only share an overlapping spectrum of activities, but also distinct functions (Benedek et al., 2017; Furukawa et al., 2016; Tilstam et al., 2017; Vincent et al., 2018). In the present study, we identified one gene-encoding DDT homolog (LjDDT) in Japanese sea bass. Without determination of complete genomic sequences, we cannot know whether the Japanese sea bass has two or more *DDT*s. Sequence comparison and phylogenetic tree analysis revealed that LjDDT was highly conserved and most closely related to the rock bream homolog. LjDDT also shared 29.2% aa identity with LjMIF, and their canonical N-terminal proline residues and enzyme activity-related sites were highly conserved. LjDDT also lacked an N-terminal signal peptide or an internal secretory sequence, thus it may be released from cells via a noncanonical protein secretion pathway, like MIF (Merk et al., 2009). The sequence similarity between LjDDT and LjMIF suggests that their biological functions may be highly correlated.

Assessment of gene expression profiles should help clarify the functionality of the *DDT* gene. In mammals, earlier studies revealed that *DDT* is constitutively expressed in rat and human tissues, with the highest level found in the liver (Nishihira et al., 1998; Zhang et al., 1995). Further studies have found that the expression of *DDT* is altered under pathological conditions. For instance, both serum protein and mRNA expression levels of *DDT* are significantly higher in burn patients compared to healthy individuals (Kim et al., 2016); whereas *DDT* mRNA expression is down-regulated in inflammatory adipose tissue in patients with wound healing disorders (Kim et al., 2017). DDT homologs in fish have also been found in many species, although their expression profiles have been rarely studied (Oh et al., 2013; Shen et al., 2012). In zebrafish, *DDT* transcripts have been detected in whole embryos throughout embryogenesis (Shen et al., 2012). In rock bream, *DDT* transcripts have been ubiquitously detected in all tested tissues, with the highest expression found in the liver, followed by blood, heart, and kidneys (Oh et al., 2013). In the present study, *LjDDT* was found to be constitutively expressed in all tested tissues of healthy Japanese sea bass, with the highest expression in the liver, consistent with previously reported results in other animals (Nishihira et al., 1998; Oh et al., 2013; Zhang et al., 1995). After *V. harveyi* infection, *LjDDT* mRNA expression was significantly down-regulated in the three tested immune tissues, i. e., liver, spleen, and head kidney. The expression profile of *LjDDT* was different to that of *LjMIF*, as determined in our previous work (Xu et al., 2019). This suggests that *LjDDT* may be functionally different from *LjMIF* , which coincides with previously described human results (Kim et al., 2017). However, the highest expression levels of *LjDDT* and *LjMIF* were all found in the liver (Xu et al., 2019), indicating that *DDT* expression is closely associated with the immune response of Japanese sea bass against *V. harveyi*.

Survival rates can intuitively reflect the degree of damage to healthy organisms caused by pathogenic infections (Fernández et al., 2018). In mammals, DDT is associated with host immunity in relation to inflammatory responses and disease severity (Merk et al., 2011; Pohl et al., 2017; Valiño-Rivas et al., 2018). For example, the administration of a specific anti-DDT antibody protects mice from lethal endotoxemia (Merk et al., 2011). In this study, we found that the administration of 10 μg/g and 100 μg/g anti-rLjDDT reduced mortality in *V. harveyi*-infected fish, but only the 100 μg/g anti-rLjDDT treatment showed statistical significance. On the other hand, the administration of 100 μg/g rLjDDT accelerated death in *V. harveyi*-infected fish. Our results coincide well with those reported previously in mice (Merk et al., 2011), suggesting that LjDDT plays a role in Japanese sea bass immunity.

Immune cell migration is a key component of many pathological processes, such as inflammation and cancer metastasis, which makes it an exciting and crucial field of study (Luster et al., 2005). MIF has a well-known chemokine-like function involving the trafficking and recruitment of macrophages and lymphocytes in vertebrates (Abe et al., 2001; Bernhagen et al., 2007; Jin et al., 2007; Schober et al., 2008; Xu et al., 2019), but there is little information on the chemotactic activity of DDT (Kim et al., 2017; Merk et al., 2011; Pasupuleti et al., 2014). DDT inhibits chemotaxis of human peripheral blood monocytes to monocyte chemoattractant protein-1 (MCP-1) (Merk et al., 2011) and functionally cooperates with MIF in promoting endothelial cell migration in the development of renal carcinoma (Pasupuleti et al., 2014). Injection of LPS combined with MIF can lead to higher peritoneal macrophage accumulation in mouse epididymal fat pads compared with the LPS-group, but with no such effect for LPS combined with DDT (Kim et al., 2017). In this study, we found that rLjDDT induced the migration of MO/MΦ and lymphocytes both *in vitro* and *in vivo*. In our previous study, we found that rLjMIF can inhibit the migration of MO/MΦ and lymphocytes (Xu et al., 2019). The opposite effect of rLjDDT and rLjMIF on immune cells suggests that they antagonistically regulate MO/MΦ and lymphocyte trafficking. MO/MΦ polarization plays an important role in modulating proinflammatory responses in fish (Lu & Chen, 2019). In teleosts, LPS from gram-negative bacteria can induce M1 polarization and cAMP can induce M2 polarization (Joerink et

al., 2006). In this study, we investigated the chemotactic activity of rLjDDT on polarized Japanese sea bass MO/MΦ. We found that rLjDDT exhibited chemotactic activity for LPS-stimulated M1-type MO/MΦ, but not for cAMP-stimulated M2-type MO/MΦ. As M1 macrophages are proinflammatory (Wang et al., 2019), our results suggest that LjDDT may be involved in the proinflammatory responses of Japanese sea bass.

The receptor mechanisms by which MIF activates target cells have long been unclear. MIF is known to not only interact with CD74, but also bind to CXCR2 and CXCR4 (Klasen et al., 2014; Presti et al., 2018; Schwartz et al., 2009; Soppert et al., 2018; Weber et al., 2008). MIF participates in the recruitment of many cell types via CXCR4 (Pawig et al., 2015). CD74 can form functional complexes with CXCR4 to mediate MIF-specific signaling (Schwartz et al., 2009). DDT also binds to CD74 with high affinity (Merk et al., 2011), but lacks the essential motif for binding to CXCR2 (Merk et al., 2012). In this study, compared with normal and MsiRNA groups, the knockdown of *LjCD74* expression in MO/MΦ significantly decreased the rLjDDT-enhanced migration of MO/MΦ, and relieved the rLjMIF-inhibited migration of MO/MΦ. The knockdown of *LjCXCR4* had no significant influence on rLjDDT-enhanced or rLjMIF-inhibited migration of MO/MΦ. The combination treatment of rLjDDT+rLjMIF had no significant effect on the migration of normal, MsiRNA, LjCD74si, or LjCXCR4si-treated MO/MΦ. This suggests that LjDDT and LjMIF have an antagonistic effect on the migration of Japanese sea bass MO/MΦ through the mediation of *LjCD74*, but not of *LjCXCR4*.

In conclusion, we characterized a DDT gene from Japanese sea bass. Upon *V. harveyi* infection, the *LjDDT* expression profiles were significantly altered in immune tissues. Antibody neutralization of LjDDT had protective effects on the survival rate of *V. harveyi*-infected Japanese sea bass. *In vivo* and *in vitro* studies revealed that LjDDT participates in the immune response by mediating the trafficking of lymphocytes and resting and M1-type MO/MΦ. After knocking down the expression of *LjCD74*, the chemotaxis of rLjDDT on MO/MΦ decreased significantly. Our present work investigated the primary role of LjDDT in Japanese sea bass immune responses. Further studies on the precise chemotactic mechanism of LjDDT and LjMIF release in response to pathogenic infections should provide insight into their immunological functions.

SUPPLEMENTARY DATA

Supplementary data to this article can be found online.

COMPETING INTERESTS

The authors declare that they have no competing interests.

AUTHORS' CONTRIBUTIONS

J.C. and M.Y.L. drafted the experiments; F.X. performed the experiments. F. X. and J. C. analyzed the data and wrote the paper. All authors read and approved the final version of the manuscript.

REFERENCES

Abe R, Peng T, Sailors J, Bucala R, Metz CN. 2001. Regulation of the CTL response by macrophage migration inhibitory factor. *The Journal of Immunology*, **166**(2): 747−753.

Benedek G, Meza-Romero R, Jordan K, Zhang Y, Nguyen H, Kent G, Li J, Siu E, Frazer J, Piecychna M, Du X, Sreih A, Leng L, Wiedrick J, Caillier SJ, Offner H, Oksenberg JR, Yadav V, Bourdette D, Bucala R, Vandenbark AA. 2017. MIF and D-DT are potential disease severity modifiers in male MS subjects. *Proceedings of the National Academy of Sciences of the United States of America*, **114**(40): E8421−E8429.

Bernhagen J, Krohn R, Lue H, Gregory JL, Zernecke A, Koenen RR, Dewor M, Georgiev I, Schober A, Leng L, Kooistra T, Fingerle-Rowson G, Ghezzi P, Kleemann R, McColl SR, Bucala R, Hickey MJ, Weber C. 2007. MIF is a noncognate ligand of CXC chemokine receptors in inflammatory and atherogenic cell recruitment. *Nature Medicine*, **13**(5): 587−596.

Bloom BR, Bennett B. 1966. Mechanism of a reaction in vitro associated with delayed-type hypersensitivity. *Science*, **153**(3731): 80−82.

Chen F, Lu XJ, Nie L, Ning YJ, Chen J. 2018. Molecular characterization of a CC motif chemokine 19-like gene in ayu (*Plecoglossus altivelis*) and its role in leukocyte trafficking. *Fish and Shellfish Immunology*, **72**: 301−308.

Chen J, Chen Q, Lu XJ, Li CH. 2014. LECT2 improves the outcomes in ayu with *Vibrio anguillarum* infection via monocytes/macrophages. *Fish and Shellfish Immunology*, **41**(2): 586−592.

Chen K, Shi YH, Chen J, Li MY. 2019. A soluble FcγR homolog inhibits IgM antibody production in ayu spleen cells. *Zoological Research*, **2019, 40**(5): 404−415.

Coleman AM, Rendon BE, Zhao M, Qian MW, Bucala R, Xin D, Mitchell RA. 2008. Cooperative regulation of non-small cell lung carcinoma angiogenic potential by macrophage migration inhibitory factor and its homolog, D-dopachrome tautomerase. *The Journal of Immunology*, **181**(4): 2330−2337.

David JR. 1966. Delayed hypersensitivity *in vitro*: its mediation by cell-free substances formed by lymphoid cell-antigen interaction. *Proceedings of the National Academy of Sciences of the United States of America*, **56**(1): 72−77.

Esumi N, Budarf M, Ciccarelli L, Sellinger B, Kozak CA, Wistow G. 1998. Conserved gene structure and genomic linkage for D-dopachrome tautomerase (DDT) and MIF. *Mammalian Genome*, **9**(9): 753−757.

Fagone P, Mazzon E, Cavalli E, Bramanti A, Petralia MC, Mangano K, Al-Abed Y, Bramati P, Nicoletti F. 2018. Contribution of the macrophage migration inhibitory factor superfamily of cytokines in the pathogenesis of preclinical and human multiple sclerosis: in silico and in vivo evidences. *Journal of Neuroimmunology*, **322**: 46−56.

Fernández J, Acevedo J, Wiest R, Gustot T, Amoros A, Deulofeu C, Reverter E, Martínez J, Saliba F, Jalan R, Welzel T, Pavesi M, Hernández-Tejero M, Ginès P, Arroyo V. 2018. Bacterial and fungal infections in acute-on-chronic liver failure: prevalence, characteristics and impact on prognosis. *Gut*, **67**(10): 1870−1880.

Furukawa R, Tamaki K, Kaneko H. 2016. Two macrophage migration inhibitory factors regulate starfish larval immune cell chemotaxis. *Immunology and Cell Biology*, **94**(4): 315−321.

Günther S, Fagone P, Jalce G, Atanasov AG, Guignabert C, Nicoletti F. 2019. Role of MIF and D-DT in immune-inflammatory, autoimmune, and chronic respiratory diseases: from pathogenic factors to therapeutic targets.

Drug Discovery Today, **24**(2): 428−439.

Guo D, Guo J, Yao J, Jiang K, Hu J, Wang B, Liu H, Sun W, Jiang X. 2016. D-dopachrome tautomerase is over-expressed in pancreatic ductal adenocarcinoma and acts cooperatively with macrophage migration inhibitory factor to promote cancer growth. *International Journal of Cancer*, **139**(9): 2056−2067.

Jankauskas SS, Wong DWL, Bucala R, Djudjaj S, Boor P. 2019. Evolving complexity of MIF signaling. *Cellular Signalling*, **57**: 76−88.

Jin HJ, Xiang LX, Shao JZ. 2007. Molecular cloning and identification of macrophage migration inhibitory factor (MIF) in teleost fish. *Developmental and Comparative Immunology*, **31**(11): 1131−1144.

Joerink M, Ribeiro CMS, Stet RJM, Hermsen T, Savelkoul HFJ, Wiegertjes GF. 2006. Head kidney-derived macrophages of common carp (*Cyprinus carpio* L. *) show plasticity and functional polarization upon differential stimulation. The Journal of Immunology*, **177**(1): 61−69.

Kim BS, Stoppe C, Grieb G, Leng L, Sauler M, Assis D, Simons D, Boecker AH, Schulte W, Piecychna M, Hager S, Bernhagen J, Pallua N, Bucala R. 2016. The clinical significance of the MIF homolog d-dopachrome tautomerase (MIF-2) and its circulating receptor (sCD74) in burn. *Burns*, **42**(6): 1265−1276.

Kim BS, Tilstam PV, Hwang SS, Simons D, Schulte W, Leng L, Sauler M, Ganse B, Averdunk L, Kopp R, Stoppe C, Bernhagen J, Pallua N, Bucala R. 2017. D-dopachrome tautomerase in adipose tissue inflammation and wound repair. *Journal of Cellular and Molecular Medicine*, **21**(1): 35−45.

Klasen C, Ohl K, Sternkopf M, Shachar I, Schmitz C, Heussen N, Hobeika E, Levit-Zerdoun E, Tenbrock K, Reth M, Bernhagen J, El Bounkari O. 2014. MIF promotes B cell chemotaxis through the receptors CXCR4 and CD74 and ZAP-70 signaling. *The Journal of Immunology*, **192**(11): 5273−5284.

Kumar S, Stecher G, Tamura K. 2016. MEGA7: Molecular evolutionary genetics analysis version7.0 for bigger datasets. *Molecular Biology and Evolution*, **33**(7): 1870−1874.

Leng L, Bucala R. 2006. Insight into the biology of macrophage migration inhibitory factor (MIF) revealed by the cloning of its cell surface receptor. *Cell Research*, **16**(2): 162−168.

Liu H, Lu XJ, Chen J. 2018. Full-length and a smaller globular fragment of adiponectin have opposite roles in regulating monocyte/macrophage functions in ayu, *Plecoglossus altivelis*. *Fish and Shellfish Immunology*, **82**: 319−329.

Lu XJ, Chen J. 2019. Specific function and modulation of teleost monocytes/ macrophages: polarization and phagocytosis. *Zoological Research*, **40**(3): 146−150.

Luster AD, Alon R, von Andrian UH. 2005. Immune cell migration in inflammation: present and future therapeutic targets. *Nature Immunology*, **6**(12): 1182−1190.

Ma Y, Su KN, Pfau D, Rao VS, Wu X, Hu X, Leng L, Du X, Piecychna M, Bedi K, Campbell SG, Eichmann A, Testani JM, Margulies KB, Bucala R, Young LH. 2019. Cardiomyocyte d-dopachrome tautomerase protects against heart failure. *The Journal of Clinical Investigation Insight*, **4**(17): 128900.

Merk M, Baugh J, Zierow S, Leng L, Pal U, Lee SJ, Ebert AD, Mizue Y, Trent JO, Mitchell R, Nickel W, Kavathas PB, Bernhagen J, Bucala R. 2009. The golgi-associated protein p115 mediates the secretion of macrophage migration inhibitory factor. *The Journal of Immunology*, **182**(11): 6896−6906.

Merk M, Mitchell RA, Endres S, Bucala R. 2012. D-dopachrome tautomerase (D-DT or MIF-2): doubling the MIF cytokine family. *Cytokine*, **59**(1): 10−17.

Merk M, Zierow S, Leng L, Das R, Du X, Schulte W, Fan J, Lue H, Chen Y, Xiong H, Chagnon F, Bernhagen J, Lolis E, Mor G, Lesur O, Bucala R. 2011. The D-dopachrome tautomerase (DDT) gene product is a cytokine and functional homolog of macrophage migration inhibitory factor (MIF). *Proceedings of the National Academy of Sciences of the United States of America*, **108**(34): E577−E585.

Nishihira J, Fujinaga M, Kuriyama T, Suzuki M, Sugimoto H, Nakagawa A, Tanaka I, Sakai M. 1998. Molecular cloning of human D-dopachrome tautomerase cDNA: N-terminal proline is essential for enzyme activation. *Biochemical and Biophysical Research Communications*, **243**(2): 538−544.

Odh G, Hindemith A, Rosengren AM, Rosengren E, Rorsman H. 1993. Isolation of a new tautomerase monitored by the conversion of D-dopachrome to 5,6-dihydroxyindole. *Biochemical and Biophysical Research Communications*, **197**(2): 619−624.

Oh M, Kasthuri SR, Wan Q, Bathige SDNK, Whang I, Lim BS, Jung HB, Oh MJ, Jung SJ, Kim SY, Lee J. 2013. Characterization of MIF family proteins: MIF and DDT from rock bream, *Oplegnathus fasciatus*. *Fish and Shellfish Immunology*, **35**(2): 458−468.

Pasupuleti V, Du W, Gupta Y, Yeh IJ, Montano M, Magi-Galuzzi C, Welford SM. 2014. Dysregulated D-dopachrome tautomerase, a hypoxia-inducible factor-dependent gene, cooperates with macrophage migration inhibitory factor in renal tumorigenesis. *Journal of Biological Chemistry*, **289**(6): 3713−3723.

Pawig L, Klasen C, Weber C, Bernhagen J, Noels H. 2015. Diversity and inter-connections in the CXCR4 chemokine receptor/ligand family: molecular perspectives. *Frontiers in Immunology*, **6**: 429.

Pohl J, Hendgen-Cotta UB, Stock P, Luedike P, Rassaf T. 2017. Elevated MIF-2 levels predict mortality in critically ill patients. *Journal of Critical Care*, **40**: 52−57.

Presti M, Mazzon E, Basile MS, Petralia MC, Bramanti A, Colletti G, Bramanti P, Nicoletti F, Fagone P. 2018. Overexpression of macrophage migration inhibitory factor and functionally-related genes, D-DT, CD74, CD44, CXCR2 and CXCR4, in glioblastoma. *Oncology Letters*, **16**(3): 2881−2886.

Rajasekaran D, Gröning S, Schmitz C, Zierow S, Drucker N, Bakou M, Kohl K, Mertens A, Lue H, Weber C, Xiao A, Luker G, Kapurniotu A, Lolis E, Bernhagen J. 2016. Macrophage migration inhibitory factor-CXCR4 receptor interactions: evidence for partial allosteric agonism in comparison with CXCL12 chemokine. *Journal of Biological Chemistry*, **291**(30): 15881−15895.

Ren Y, Liu SF, Nie L, Cai SY, Chen J. 2019. Involvement of ayu NOD2 in NF-κB and MAPK signaling pathways: insights into functional conservation of NOD2 in antibacterial innate immunity. *Zoological Research*, **40**(2): 77−88.

Rijvers L, Melief MJ, van der Vuurst de Vries RM, Stéphant M, van Langelaar J, Wierenga-Wolf AF, Hogervorst JM, Geurts-Moespot AJ, Sweep FCGJ, Hintzen RQ, van Luijn MM. 2018. The macrophage migration inhibitory factor pathway in human B cells is tightly controlled and dysregulated in multiple sclerosis. *European Journal of Immunology*, **48**(11): 1861−1871.

Schober A, Bernhagen J, Weber C. 2008. Chemokine-like functions of MIF in atherosclerosis. *Journal of Molecular Medicine*, **86**(7): 761−770.

Schwartz V, Lue H, Kraemer S, Korbiel J, Krohn R, Ohl K, Bucala R, Weber C, Bernhagen J. 2009. A functional heteromeric MIF receptor formed by CD74 and CXCR4. *FEBS Letters*, **583**(17): 2749−2757.

Shen YC, Thompson DL, Kuah MK, Wong KL, Wu KL, Linn SA, Jewett EM, Shu-Chien AC, Barald KF. 2012. The cytokine macrophage migration inhibitory factor (MIF) acts as a neurotrophin in the developing inner ear of the zebrafish, *Danio rerio*. *Developmental Biology*, **363**(1): 84−94.

Sinitski D, Kontos C, Krammer C, Asare Y, Kapurniotu A, Bernhagen J. 2019. Macrophage migration inhibitory factor (MIF)-based therapeutic concepts in atherosclerosis and inflammation. *Journal of Thrombosis and Haemostasis*, **119**(4): 553−566.

Soppert J, Kraemer S, Beckers C, Averdunk L, Möllmann J, Denecke B, Goetzenich A, Marx G, Bernhagen J, Stoppe C. 2018. Soluble CD74 reroutes MIF/CXCR4/AKT-mediated survival of cardiac myofibroblasts to necroptosis. *Journal of the American Heart Association*, **7**(17): e009384.

Sugimoto H, Taniguchi M, Nakagawa A, Tanaka I, Suzuki M, Nishihira J. 1999. Crystal structure of human D-dopachrome tautomerase, a homologue of macrophage migration inhibitory factor, at1.54 Å resolution. *Biochemistry*, **38**(11): 3268−3279.

Tilstam PV, Qi D, Leng L, Young L, Bucala R. 2017. MIF family cytokines in cardiovascular diseases and prospects for precision-based therapeutics. *Expert Opinion on Therapeutic Targets*, **21**(7): 671−683.

Valiño-Rivas L, Cuarental L, Grana O, Bucala R, Leng L, Sanz A, Gomez G, Ortiz A, Sanchez-Niño MD. 2018. TWEAK increases CD74 expression and sensitizes to DDT proinflammatory actions in tubular cells. *PLoS One*, **13**(6): e0199391.

Vincent FB, Lin E, Sahhar J, Ngian GS, Kandane-Rathnayake R, Mende R, Hoi AY, Morand EF, Lang T, Harris J. 2018. Analysis of serum macrophage migration inhibitory factor and D-dopachrome tautomerase in systemic sclerosis. *Clinical & Translational Immunology*, **7**(12): e1042.

Wang LX, Zhang SX, Wu HJ, Rong XL, Guo J. 2019. M2b macrophage polarization and its roles in diseases. *Journal of Leukocyte Biology*, **106**(2): 345−358.

Wang Q, Wei Y, Zhang J. 2017. Combined knockdown of D-dopachrome tautomerase and migration inhibitory factor inhibits the proliferation, migration, and invasion in human cervical cancer. *International Journal of Gynecological Cancer*, **27**(4): 634−642.

Weber C, Kraemer S, Drechsler M, Lue H, Koenen RR, Kapurniotu A, Zernecke A, Bernhagen J. 2008. Structural determinants of MIF functions in CXCR2-mediated inflammatory and atherogenic leukocyte recruitment. *Proceedings of the National Academy of Sciences of the United States of America*, **105**(42): 16278−16283.

Xu F, Shi YH, Chen J. 2019. Characterization and immunologic functions of the macrophage migration inhibitory factor from Japanese sea bass, *Lateolabrax japonicus*. *Fish and Shellfish Immunology*, **86**: 947−955.

Yu L, Li CH, Chen J. 2019. A novel CC chemokine ligand 2 like gene from ayu *Plecoglossus altivelis* is involved in the innate immune response against to *Vibrio anguillarum*. *Fish and Shellfish Immunology*, **87**: 886−896.

Zhang M, Åman P, Grubb A, Panagopoulos I, Hindemith A, Rosengren E, Rorsman H. 1995. Cloning and sequencing of a cDNA encoding rat D-dopachrome tautomerase. *FEBS Letters*, **373**(3): 203−206.

Zhou QJ, Wang L, Chen J, Wang RN, Shi YH, Li CH, Zhang DM, Yan XJ, Zhang YJ. 2014. Development and evaluation of a real-time fluorogenic loop-mediated isothermal amplification assay integrated on a microfluidic disc chip (on-chip LAMP) for rapid and simultaneous detection of ten pathogenic bacteria in aquatic animals. *Journal of Microbiological Methods*, **104**: 26−35.